

# Tunable Metamaterial-Inspired Resonators for Optimal Wireless Power Transfer Schemes

A. X. Lalas<sup>1</sup>, N. V. Kantartzis<sup>1</sup>, T. T. Zygoridis<sup>2</sup>, T. P. Theodoulidis<sup>3</sup>

1. Dept. of Electrical & Comp. Engineering, Aristotle Univ. of Thessaloniki, Thessaloniki 54124, Greece

2. Dept. of Informatics & Telecomm. Engineering, Univ. of Western Macedonia, Kozani 50100, Greece

3. Dept. of Mechanical Engineering, Univ. of Western Macedonia, Kozani 50100, Greece

**Abstract –** A consistent methodology for the precise design and realization of electromagnetic resonance-based wireless power transfer (WPT) systems through various metamaterial-oriented forms is presented in this paper. To this goal, an assortment of resonating elements is chosen, like the edge-coupled split ring resonator (EC-SRR) or the E2 SRR. Specifically, the macroscopic properties of these elements are accurately retrieved and the prior SRRs are then incorporated in the featured WPT scheme, also in the form of a metasurface. All results and designs are obtained via the COMSOL Multiphysics® software. The performance of the systems, including the magnetically resonant SRR, is found to be promising for distances within a few centimeters, as anticipated from the initial theoretical analysis, in contrast to the scenario of the electrically resonant elements.

## Introduction

The emergence of wireless power transfer (WPT) technology has offered a gradually evolving research field with a multitude of triggering applications, like electric vehicles, bio-medical implants and wireless charging media for consumer electronics. However, since the initial establishment of its principal characteristics, instructive WPT efficiencies have been implemented only for rather small distances [1]-[3]. Research on this issue has revealed that WPT through electromagnetic resonance can achieve a relatively high efficiency, when these circuits share the same resonance, while the relation between the coupling coefficient and total losses is optimal [4]. Potential candidates for the fulfillment of these requisites are the metamaterials [5], [6] – synthetically engineered media with unique electromagnetic properties, not available in nature – on condition that a wide bandwidth is provided. For the latter attribute, numerous mechanisms have been utilized to accomplish radical bandwidth reconfigurability [7]-[9].

Typical metamaterials, employed for this purpose, are various types of split-ring resonators (SRRs). Such configurations offer a negative effective relative permeability within a spectrum above their resonance frequency, when excited by a suitably oriented external electric/magnetic field. Hence, a magnetic reso-

nance that increases the magnetic coupling between the SRRs is generated [10]-[12]. Other types of SRRs have been, also, devised to eliminate any magnetic properties, thus leading to electric resonators with negative effective permittivity [13]. As WPT is accomplished in terms of the magnetic coupling of the equivalent coils of two resonators, elements with pure electric properties above their resonance frequency are not expected to drastically improve the efficiency of the system. Nevertheless, the necessity of compactness in modern technology opts for further miniaturization of such structures to enable portability.

Based on the above aspects, a class of metamaterial resonators is launched in this paper for the significant efficiency improvement of contemporary WPT topologies. Furthermore, the incorporation of programmable edge-coupled SRRs (EC-SRRs) and E2 SRRs [6], in the form of periodic metasurfaces, which can mitigate proximity effects when interacting with the source and load loops, is thoroughly investigated. Essentially, the metasurface operates as the resonator of the featured device, guaranteeing increased levels of efficiency. In this way, the proposed design methodology retrieves the optimal dimensions and electromagnetic parameters of the aforementioned metamaterial-based forms in order to provide advanced levels of WPT efficiency. The performance of every setup is numerically extracted and assessed by means of the COMSOL Multiphysics® computational package (simulations are conducted via the RF module) [14], which implements the finite element method (FEM). In particular, the impact of the different system parameters (metamaterial dimensions, distance between the resonators, and distance between each SRR and the corresponding coil) on the overall performance is comprehensively explored. Additionally, a variety of optimally-designed laboratory prototypes has been fabricated to facilitate the appropriate comparisons in terms of realistic operation conditions. Numerical results and comparisons with measured data substantiate the advantages of the analysis and support our concept for the profitable use of controllable metamaterial-based arrangements in cutting-edge WPT systems.

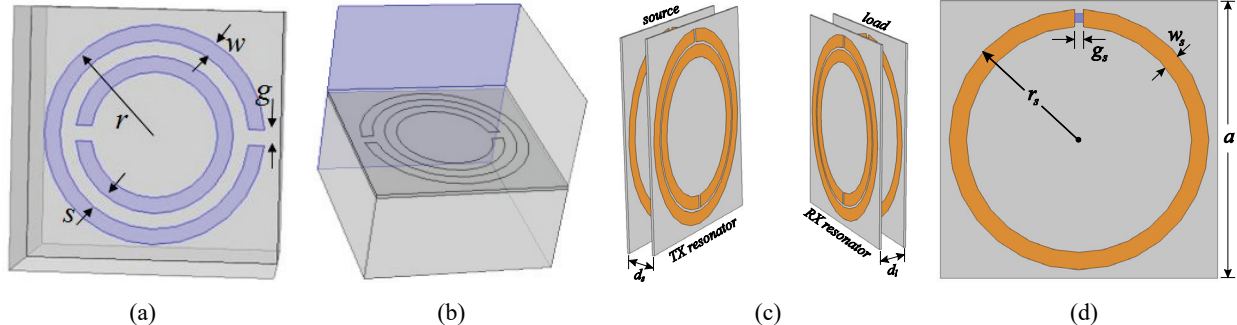


**Figure 1.** Geometry of (a) the EC-SRR and (b) the unit cell for the retrieval of the EC-SRR effective constitutive parameters via the COMSOL Multiphysics® software. The blue face of the cell is related to the electric excitation, which generates the magnetic resonance of the EC-SRR structure. Depiction of (c) the metamaterial-inspired WPT system and (d) the source loop.

### Theoretical Study of the EC-SRR Setup

The optimal working frequency of a WPT system in the case of SRRs as its resonating elements is within the spectrum of magnetic resonance, namely an excitation frequency that generates the appearance of a negative effective permeability. In essence, this spectrum is located slightly above the frequency where the SRR equivalent reactance is equal to zero (resonance frequency). Consequently, the optimal working frequency of the WPT system can be theoretically estimated, if the resonance frequency is known. Specifically, the confinement of the electric field between the narrow gap, formed by the two rings of the EC-SRR, as shown in Fig. 1(a), is deemed decisive for the minimization of any interaction with adjacent structures. Hence, a WPT system can be designed by considering the prior EC-SRRs as its transmitting (Tx) and receiving (Rx) components.

Prior to delving in the proposed metamaterial-enabled WPT system, we thoroughly investigate the resonance frequency behavior of the EC-SRR in Fig. 1(a), with the typical dimensions of  $r = 35$  mm and  $w = g = s = 5$  mm. Therefore, we extract the shift of the resonance frequency for different dimensions and dielectric slab properties. Next, these SRRs are placed as resonators in the featured WPT arrangement, which is excited at the region of the estimated optimal frequency, with the expectation to exhibit a high performance in this region. To this aim, a parametric sweep for various dimensions or media characteristics unveils the notable stability of the efficiency level under changes in the environment of the system and certifies the merits of the design technique.

Our analysis starts by following the approach of [5] and [6], which establishes a means for the computation of the equivalent EC-SRR inductance, created by the rings, and the equivalent capacitance, due to the gap  $s$  between the internal and external ring. According to this scheme, given the inductance and capacitance, the resonance frequency can be evaluated

**Table 1:** Resonances of the featured unit cell

Unit cell characteristics		Resonance frequency (MHz)
Substrate relative permittivity	EC-SRR gap	
$\epsilon_r = 2.21$	$s = 5$ mm	508
$\epsilon_r = 4.5$	$s = 5$ mm	437
$\epsilon_r = 4.5$	$s = 3$ mm	379
$\epsilon_r = 4.5$	$s = 1$ mm	300

as  $f_r = 1/[2\pi(LC)^{1/2}]$ . An optimal set of such theoretically-derived results, for  $w = 5$  mm, is summarized in Table 1. As observed, the decrease of  $s$  leads to an inevitable shift of the resonance to lower frequencies, mainly attributed to the higher equivalent capacitance. Also, the permittivity of the dielectric slab has a decent effect on the resonance frequency. So, an EC-SRR resonator with a desirable frequency response and range may be designed through the proper selection of the aforesaid parameters. In this manner, the necessity of lossy external capacitances at the gap of each ring for the adjustment of the SRR frequency response, is avoided.

The next step of our formulation retrieves the optimal values of the EC-SRR effective constitutive parameters,  $\epsilon_{eff}$  and  $\mu_{eff}$ , through the COMSOL Multiphysics® computational suite (and its RF module) [14]. The configuration for this objective, schematically given in Fig. 1(b), is a unit cell with the appropriate boundary conditions and excitation process, equivalent to an infinite plane, where the EC-SRRs are periodically placed with a period of  $a$ . The  $S$ -parameters, derived from these numerical simulations, are additionally processed through a well-known homogenization function [15], [16], in order to finally derive the required  $\epsilon_{eff}$  and  $\mu_{eff}$  for the selected excitation frequencies, as illustrated in the plots of Fig. 2. It is noteworthy to stress that all approaches provided similar and reliable outcomes.

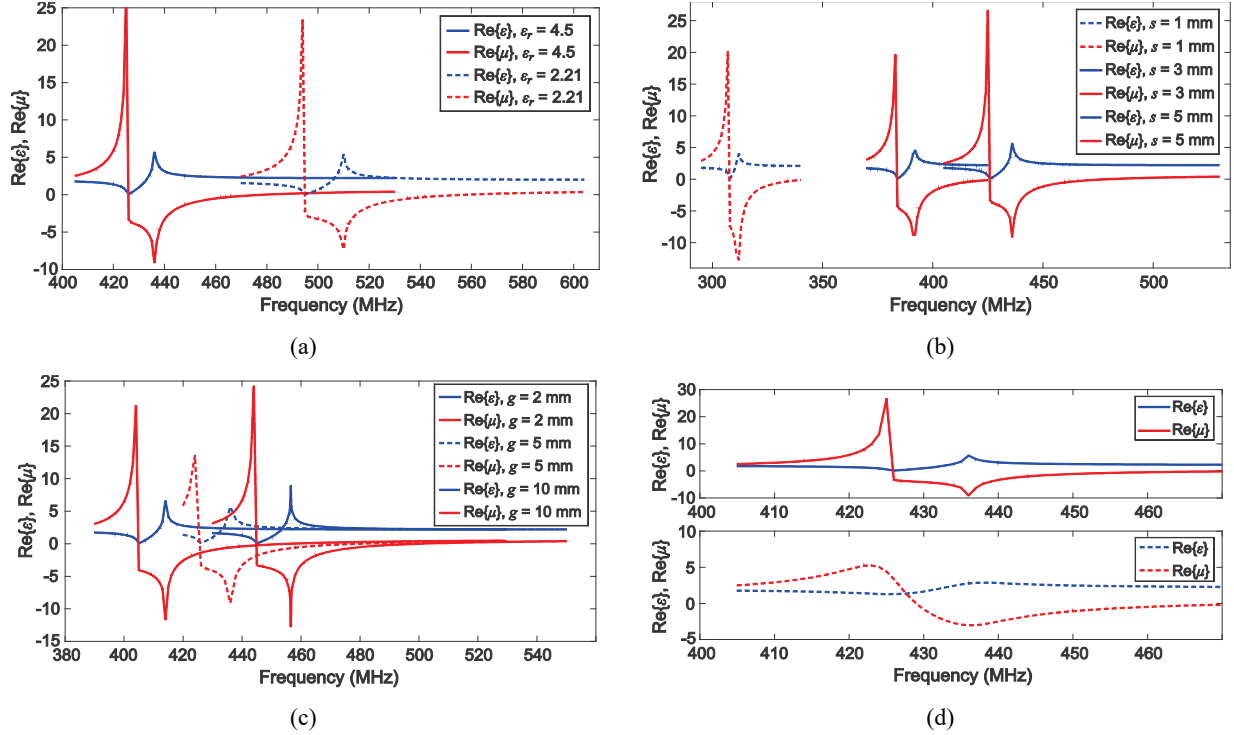


**Figure 2.** Real parts of the EC-SRR effective constitutive parameters as a function of the operating frequency, for diverse dimensions and substrate characteristics, acquired via the COMSOL Multiphysics® software. (a)  $\epsilon_r$ , (b)  $s$ , (c)  $g$ , and (d) lossless and lossy (FR4;  $\sigma = 0.004 \text{ S/m}$ ) substrate with the same  $\epsilon_r = 4.5$ .

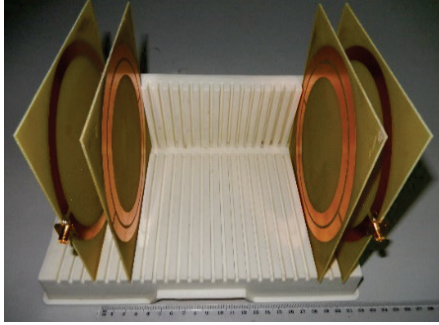


**Figure 3.** Fabricated prototype of the designed metamaterial-based WPT system.

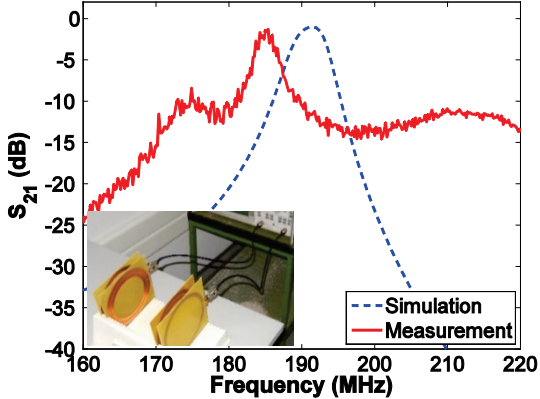
### The metamaterial-inspired WPT system

The featured WPT scheme, described in Fig. 1(c), replaces the typical transmitter and receiver coils of existing implementations with EC-SRRs. Furthermore, its fabricated prototype is presented in Fig. 3. Except for the resonators, a source loop and a load loop are necessary, while the dimensions of the copper resonator are:  $r = 75 \text{ mm}$ ,  $w = 10 \text{ mm}$ ,  $s = 2 \text{ mm}$ , and  $g = 2.5 \text{ mm}$ . In addition, the cell period is  $a = 160 \text{ mm}$  and the thickness of the Taconic™ TLY5 substrate is  $1.5748 \text{ mm}$ . On the other hand, the design parameters of the source loop, illustrated in Fig. 1(d), are  $r_s = 75 \text{ mm}$ ,  $w_s = 10 \text{ mm}$ , and  $g_s = 5 \text{ mm}$ . The

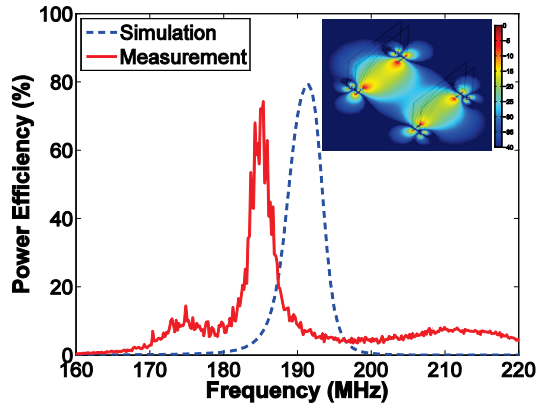
distance between the source loop and the Tx resonator as well as between the load loop and the Rx resonator are  $d_s = 20 \text{ mm}$  and  $d_l = 20 \text{ mm}$ , respectively. It should be emphasized that the system components are aligned along a straight line, whereas the distance between the Tx and Rx resonators is set to  $d = 150 \text{ mm}$ . Additionally, the system is excited at a frequency spectrum in the vicinity of the metamaterial's magnetic resonance. Note that although the frequencies computed in the previous subsections concern an infinite plane of EC-SRRs, only a negligible divergence is expected to appear in the results.

In this framework, we take avail of the RF module in the COMSOL Multiphysics® computational suite to extract our results, whereas all measurements, associated to the fabricated prototype of Fig. 3, are collected via a vector network analyzer. A performance assessment is presented in Fig. 4, providing experimental validation and revealing the benefits of the new system. The slight frequency shift between simulation and measurement data, is mainly attributed to inevitable imperfections during the fabrication process. However, it remains at a very acceptable level.

Subsequently, to examine the sensitivity and the efficiency of our WPT system in terms of changes in dimensions and media parameters, we conduct a detailed parametric study in Fig. 5. As detected, the highest efficiency occurs at a frequency slightly above



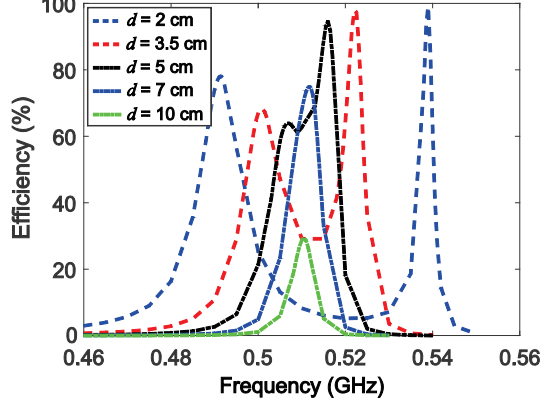
(a)



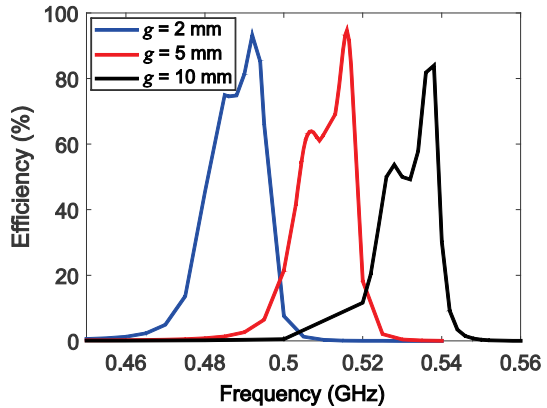
(b)

**Figure 4.** Performance of the proposed metamaterial-based WPT device in terms of (a) the  $S_{21}$ -parameter (inlet photo: measurement setup), (b) power efficiency (inlet surface plot: magnetic field intensity (in dB) at 191 MHz).

the magnetic resonance spectrum for every case. For instance, regarding an initial set of parameters:  $w = g = s = 5$  mm,  $d = 5$  cm, and  $\alpha = 8$  cm, the optimal working frequency is found to be 516 MHz, while the magnetic resonance has been calculated in the range of 426–478 MHz. This slight divergence is basically attributed to the fact that all unit cell simulations analyze the scenario of an infinite plane of EC-SRRs, whose interactions decreases the resonant frequency. It can be, also, observed in Fig. 5(a) that the efficiency of our setup is very satisfactory for the majority of the examined cases, exceeding the level of 80% or even reaching the promising value of 99.03% for  $d = 2$  cm. Hence, the designed structure is deemed suitable for small and medium distances (up to 7 cm) for the specific EC-SRR dimensions. Overall, it is stated that despite the somewhat confined distance values, the specific realization can be reliably used in many contemporary applications, such as miniaturized communication devices and high-end electronic components.



(a)



(b)

**Figure 5.** Efficiency of the proposed metamaterial-based WPT system for various EC-SRR and substrate parameters. (a)  $d$  and (b)  $g$ .

To further verify our design methodology, we examine the E2 SRR configuration of Fig. 6(a), similar to the EC-SRR one. Nonetheless, due to its increased complexity, there is not any analytical formula for the theoretical calculation of its resonance frequency. So, the analysis of the specific WPT system will solely rely on unit cell simulations, which have been proven very trustworthy. To this end, the main dimensions of the structure are  $D_1 = 57.6$  mm,  $D_2 = 51.2$  mm,  $l_1 = 19.2$  mm,  $l_2 = 20$  mm, and  $\alpha = 8$  cm, whereas the dielectric substrate is lossless with  $\epsilon_r = 4.5$ . The structure for the computation of the E2 SRR effective constitutive parameters is shown in Fig. 6(b). Basically, for this kind of SRR, there are two polarizations (i.e. horizontal and vertical) [16] for the external electric field excitation, which lead to different system responses. Therefore, in Figs. 6(c) and 6(d), we present the results for both polarizations. It is promptly deduced that the effective permittivity can receive negative values, owing to the electric resonance of the E2 SRR.

Due to its increased complexity, the mutual E2 SRR interactions and the spectrum of its negative  $\epsilon_r$ ,

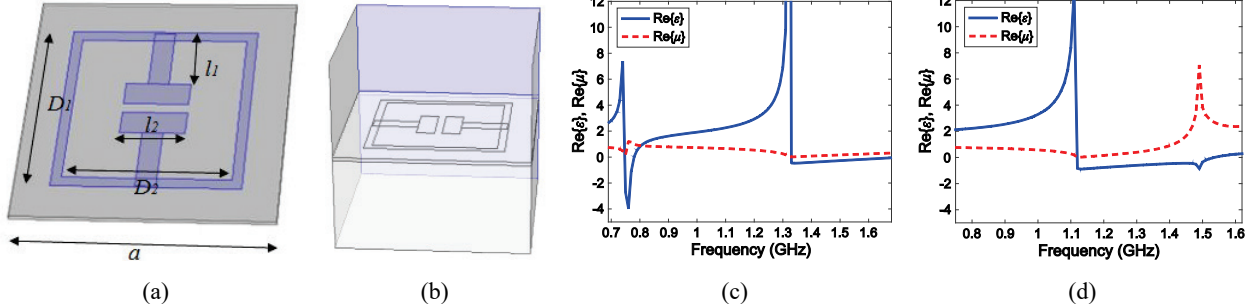
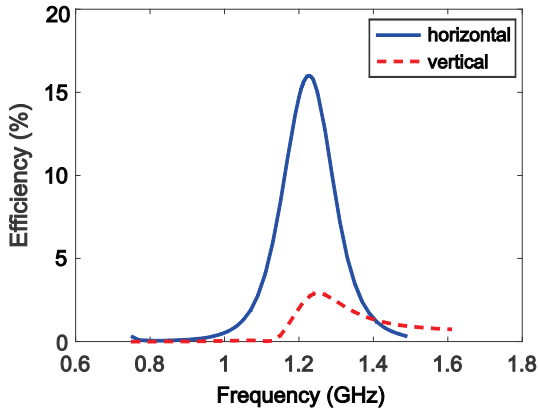
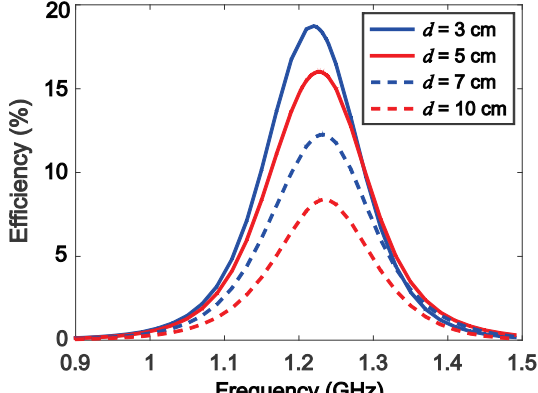


**Figure 6.** Geometry of (a) the E2 SRR and (b) the unit cell for the EC-SRR effective constitutive parameters via the COMSOL Multiphysics® software. The SRR can be excited either through the blue face (horizontal polarization) or the shaded face (vertical polarization). Effective constitutive parameters for the case of (a) a horizontally and (b) a vertically polarized excitation.



(a)

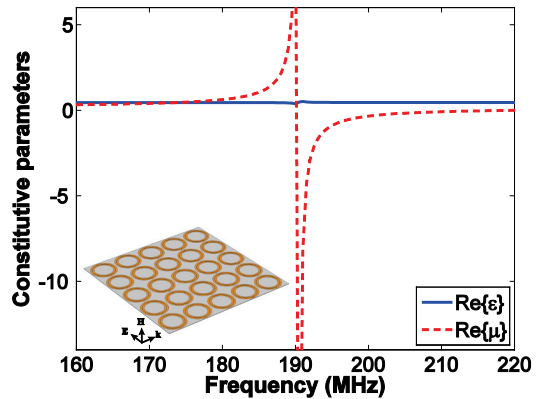


(b)

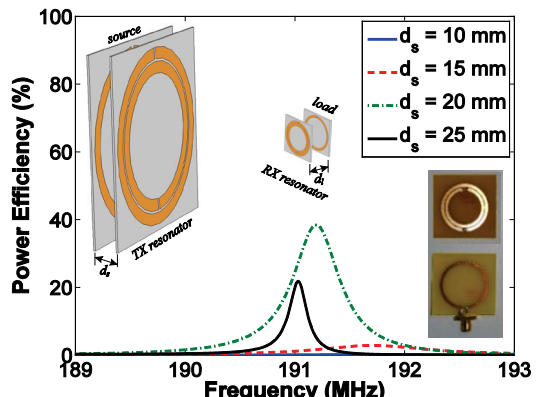
**Figure 7.** Efficiency of the alternative metamaterial-based WPT system for (a) horizontal and vertical polarization and (b) various  $d$  values. The distance of the source and load coils from the E2 SRRs is  $d_s = d_l = 5$  mm.

the particular WPT system is not expected to provide high levels of efficiency. However, this scenario has been selected to verify the performance of our algorithm in such complicated implementations. Indeed, and as Fig. 7 clarifies, the setup exhibits a rather small efficiency (not exceeding 19%), confirming our initial expectations. Specifically, the optimal working

frequency for both polarizations is around 1.2 GHz, which does not belong to the electric resonance spectrum for the horizontal polarization case. Therefore, it may be derived that when electrically resonant metamaterials are utilized, the maximum efficiency cannot be obtained at the electric resonance.

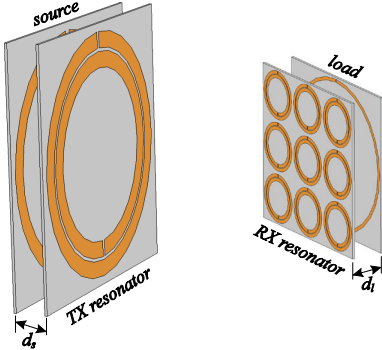


(a)

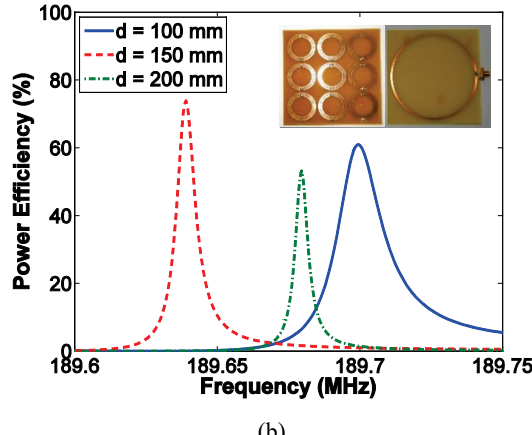


(b)

**Figure 8.** Behavior of the EC-SRR metasurface arrangement (inlet sketch: periodic metasurface) in terms of (a) the constitutive parameters real parts and (b) the power efficiency of the WPT system for various  $d_s$  (inlet sketch and photo: topology and fabricated prototype).



(a)



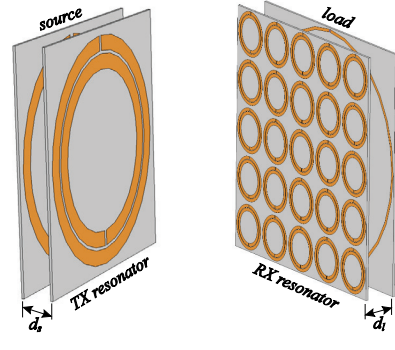
(b)

**Figure 9.** (a) Setup and (b) performance of the  $3 \times 3$  EC-SRR WPT system in terms of power efficiency for various  $d$  of the Tx-Rx components (inlet photo: fabricated prototype).

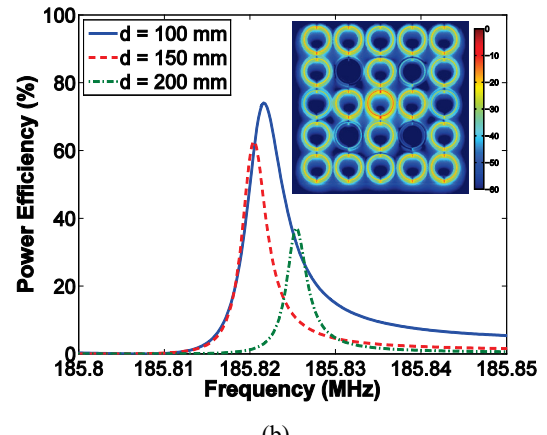
## Efficiency Enhancement via Metasurfaces

The properties of the WPT system can be additionally improved by taking avail of metasurfaces, i.e. planar periodically-repeated metamaterial structures. So, multiple topologies can be developed with tunable attributes. As compact dimensions constitute a critical issue in WPT research, our initial efforts concentrate on the minimization of the Rx component, while other setups with metasurfaces as Rx elements are explored. For this purpose, we obtain the magnitude of the  $S_{21}$ -parameters and the power transfer efficiency of the featured structures.

A compact EC-SRR (downscaled by 5) is shown in Fig. 8(a) along with the constitutive effective parameters of its periodic repetition. Furthermore, Fig. 8(b) presents a parametric study of the influence of distance  $d_s$  (distance between the source/load loop and the EC-SRR) on the WPT system. A maximum efficiency of 38.42% is attained at 191.2 MHz, when  $d_s = 20$  mm. Apparently, the behavior is degraded in comparison with the initial structure. To alleviate this issue, two discrete scenarios are investigated with  $3 \times 3$  and  $5 \times 5$



(a)



(b)

**Figure 10.** (a) Setup and (b) behavior of the  $5 \times 5$  EC-SRR WPT system in terms of power efficiency for various  $d$  of the Tx-Rx components (inlet surface plot: electric field intensity (in dB) at 185.6 MHz at the EC-SRRs surface).

downscaled EC-SRRs arrays. These devices include lumped capacitive elements of 8.3 pF to retain the selected operation frequency.

Specifically, the  $3 \times 3$  EC-SRR WPT system together with a parametric analysis of distance  $d$  between the Tx and Rx elements, are given in Fig. 9. As detected, a frequency shifting follows the variation of  $d$ . A maximum efficiency of 73.85% is acquired at 189.6 MHz, when  $d = 150$  mm. Also, an estimation for the  $5 \times 5$  EC-SRR WPT system is provided in Fig. 10, revealing a minor frequency shifting, yet large changes of power efficiency levels. Recalling Fig. 10(b), a maximum efficiency of 62.69% can be observed at 185.8 MHz, when  $d = 150$  mm.

Finally, a comparison between different structures is performed in Fig. 11(a). As detected, the total efficiency increases, when the Rx metasurface expands, but a trade-off arises regarding the useful bandwidth of power transfer and power efficiency level. A characteristic snapshot of the magnetic field intensity is displayed in Fig. 11(b) at 185.6 MHz for the  $5 \times 5$  case. One may discern that maximum values are located at the region of the central EC-SRR.

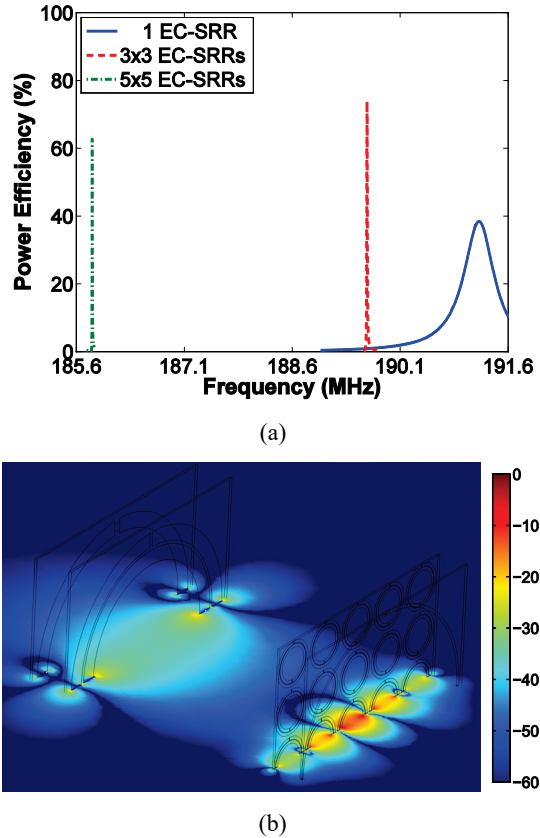


**Figure 11.** (a) Performance assessment of the EC-SRR based WPT system for various configurations and (b) magnetic field intensity (in dB) at 185.6 MHz for the 5x5 case.

## Conclusions

A systematic method for the design of WPT systems via resonant metamaterials as their transmitter and receiver, has been proposed in this paper. Two distinct SRR types, magnetically and electrically resonant, have been considered, while additional enhancement of power transfer efficiency has been accomplished by means of periodic metasurfaces. Numerical simulations, through COMSOL Multiphysics® computational package (RF module), and comparisons with measurement data (from fabricated prototypes) unveiled that since the power transfer is based on the magnetic coupling, the SRRs with the magnetic response can offer very high efficiencies for small distances at a specific operating frequency.

## References

1. A. Kurs, A. Karalis, R. Moffatt, J. D. Joannopoulos, P. Fisher, and M. Soljacic, Wireless energy transfer via strongly coupled magnetic resonances, *Science*, **317**, pp. 83–85 (2007).
2. A. Karalis, J. D. Joannopoulos, and M. Soljačić, Efficient wireless non-radiative mid-range energy transfer, *Annals Phys.*, **323**, pp. 34–48 (2008).
3. O. Jonah, S. Georgakopoulos, and M. Tentzeris, Optimal design parameters for WPT by resonance magnetic, *IEEE Antennas Wireless Propag. Lett.*, **11**, pp. 1390–1393 (2012).
4. C. J. Stevens, Magnetoinductive waves and wireless power transfer, *IEEE Trans. Power Electron.*, **30**, pp. 6182–6190 (2014).
5. R. Marqués, F. Martín, and M. Sorolla, *Metamaterials with negative parameters: Theory, design, and microwave applications*, Wiley-Interscience, New York (2008).
6. L. Solymar and E. Shamonina, *Waves in metamaterials*, Oxford University Press, Oxford (2009).
7. A. L. Ranaweera, T. P. Duong, and J. Lee, Experimental investigation of compact metamaterial for high efficiency mid-range wireless power transfer applications, *J. Appl. Phys.*, **116**, Art. ID 043914 (2014).
8. H. Kim and C. Seo, Highly efficient wireless power transfer using metamaterial slab with zero refractive property, *Electron. Lett.*, **50**, no. 16, pp. 1158–1160 (2014).
9. K. Le, H. Yuli, and Z. Wei, Experiments on multiple-receiver magnetic resonance-based wireless power transfer in low megahertz with metamaterials, *Appl. Phys. A*, **122**, pp. 373–380 (2016).
10. H. Hu and S. V. Georgakopoulos, Wireless powering based on strongly coupled magnetic resonance with SRR elements, in Proc. 2012 IEEE Antennas Propag. Soc. Int. Symp., pp. 1–2 (2012).
11. Y. Fan, L. Li, S. Yu, C. Zhu, and C. Liang, Experimental study of efficient WPT system integrating with highly sub-wavelength metamaterials, *PIERS*, **141**, pp. 769–784 (2013).
12. Y. Y. Zhang, H. Tang, C. Yao, Y. Li, and S. Xiao, Experiments on adjustable magnetic metamaterials applied in MHz wireless power transmission, *AIP Advances*, **5**, Art. ID 017142 (2015).
13. A. X. Lalas, N. V. Kantartzis, and T. D. Tsiboukis, Efficiency enhancement of metamaterial wireless energy transfer topologies, in Proc. 2016 IEEE Wireless Power Transfer Conf., pp. 1–3 (2016).
14. *COMSOL Multiphysics® Software*, COMSOL Inc., ver. 5.1 (2015).
15. X. Chen, T. M. Grzegorczyk, B. Wu, J. Pacheco, and J. Kong, Robust method to retrieve the constitutive effective parameters of metamaterials, *Phys. Rev. E*, **70**, Art. ID 016608 (2004).
16. W. Padilla, M. Aronsson, C. Highstrete, M. Lee, A. Taylor and R. Averitt, Electrically resonant THz metamaterials: Theoretical and experimental investigations, *Phys. Rev. B*, **75**, Art. ID 041102(R) (2007).